

Entanglement generation in a quantum network with finite quantum memory lifetime

Vyacheslav Semenenko

Department of Electrical Engineering, University at Buffalo, Buffalo, NY 14260, USA

Xuedong Hu

Department of Physics, University at Buffalo, Buffalo, NY 14260, USA

Eden Figueroa

Department of Physics and Astronomy, Stony Brook University, Stony Brook, NY 11794, USA

Vasili Perebeinos*

Department of Electrical Engineering, University at Buffalo, Buffalo, NY 14260, USA

(Dated: October 5, 2021)

We simulate entanglement sharing between two end-nodes of a quantum network using Se-QUeNCe, an open-source simulation package for quantum networks. Our focus is on the rate of entanglement generation between the end-nodes with many repeaters with a finite quantum memory lifetime. Our findings demonstrate that the performance of quantum connection depends highly on the entanglement management protocol scheduling entanglement generation and swapping, resulting in the final end-to-end entanglement. Numerical and analytical simulations show limits of connection performance for a given number of repeaters involved, memory lifetimes for a given distance between the end nodes, and an entanglement management protocol.

I. INTRODUCTION

In recent years much research efforts have been focused on the development of quantum communication networks [1–9]. Small linear quantum networks (with maximum distance in a pair of nodes up to about 100 km) have already been demonstrated [10, 11]. Theoretical development of network protocols has reached its third generation, which is separated against the ways of how quantum state error correction is implemented [12]. The first two generations are based on heralded entanglement generation, requiring signaling back to communicating nodes about the generation status. The third generation of the quantum network is free from this obligation that significantly limits the network throughput. However, the third generation networks make severe demands on the fidelity of quantum gates that are now incompatible with today’s hardware’s characteristics [13, 14].

Currently, available quantum hardware components are still far from allowing the realization of a fully functional first-generation network for long-distance end-to-end quantum communication [15]. Key bottlenecks include limited coherence time of qubits and photon loss in the quantum channel medium between the end-nodes. While the latter issue can, in principle, be overcome by using quantum repeaters [2, 3, 16–20], the former has been a persistent impediment to progress in quantum communication in particular and quantum information technologies in general.

Quantum memories are key ingredients for a quantum repeater [21, 22]. Their coherent lifetime is crucial to cre-

ating and maintaining high fidelity entanglement [23–25] and is dependent on the materials platform. While typical spin qubits coherence time of a few milliseconds up to a second in silicon [26, 27] and diamond [28–30] are comparable to an average ping time of about 0.1 milliseconds in classical networks, the trapped ions demonstrate memory lifetimes from several minutes to hours [31–33]. However, the frequency conversion efficiency to telecommunication wavelength ($\sim 1560 \mu\text{m}$) photon frequency remains low [34–36]. Currently, there is intense research for quantum memory development based on novel two-dimensional materials [37], rare Earth ion-doped optical fibers [38, 39], and quantum dots [40] which would operate at the telecommunication wavelength of the quantum memory developments, thus obviating the need for the frequency conversion step. The variety of materials platforms [41] for the quantum network components make the design of quantum networks a challenging engineering task. Preliminary simulations are necessary for designing optical-fiber classical connections specifically for quantum networks [42–47]. This kind of simulation allows a designer to construct the most tolerant protocol to account for classical network ping, single-photon traveling time fluctuations, and other parameter imperfections in the quantum network hardware and evaluate if the existing hardware satisfies the error-robustness requirements.

One of the essential resources for a quantum network is the entanglement between any two network nodes, which would allow the transfer of unknown states between the nodes via quantum teleportation. Many protocols have been suggested to generate such remote entanglement. For example, one protocol aims to minimize the time that each qubit spends in an entangled state during the entanglement generation and requires that all the inter-

* vasilipe@buffalo.edu

mediate links between the end nodes succeed simultaneously. Such an approach reduces the impact of qubit decoherence, but the need for synchronicity can be demanding. Another protocol relies on qubits to preserve an entangled state for a much longer time until all the links are successfully established between the end nodes. Such an approach reduces the number of attempts but requires the qubits to stay in the entangled states with high fidelity for long times [48].

Here we analyze the entanglement generation capabilities between the end-nodes in a simple linear network using SeQeNCe quantum network simulator [43, 45]. We examine the two protocols discussed above in detail, applied towards the generation of elementary links between adjacent nodes. Our results for both scenarios set the requirements on the number of repeaters and memory lifetime for different distances between the end nodes.

II. GENERATION OF THE ELEMENTARY QUANTUM LINK

An elementary link between two quantum network nodes is established when quantum entanglement is created between a pair of qubits belonging to the nodes. The entanglement, once created, is a resource used for quantum information transmission from one node to the other. Once a quantum state from the sending node is transmitted, the entanglement is destroyed. Thus, an essential parameter characterizing the performance of a given quantum connection is the maximum rate at which entanglement can be generated.

Many protocols have been proposed to generate entanglement between two qubits. Here we choose to analyze the Barrett-Kok protocol's performance [49] for entanglement generation between two nodes with and without intermediate nodes (quantum repeaters), though our analysis can be generalized to other protocols straightforwardly. An elementary link in the Barrett-Kok protocol is shown in Fig. 1. The nodes are located at a distance L from each other, and the Bell-state measuring (BSM) station is located right in the middle (in terms of the length of optical communication fiber). We assume that synchronization and scheduling instructions start with basic operations, such as single-photon emission. The instructions are obtained from a single node, called C-node (controlling node), one of the nodes forming a chain and participating in the end-to-end quantum connection. It is most efficient to assign C-node duties to the middle node in the chain, so the maximum ping to the rest nodes is minimal. In Fig. 1a, there are no intermediate nodes between the end nodes, so one is chosen as a control node. The presence of C-node makes the system hierarchic, i.e., managed from the single center that allows us to focus on the analysis of the performance of the quantum network and frees us from developing more complex communication protocols specific to peer-to-peer networks [50].

The entanglement generation is done in the following

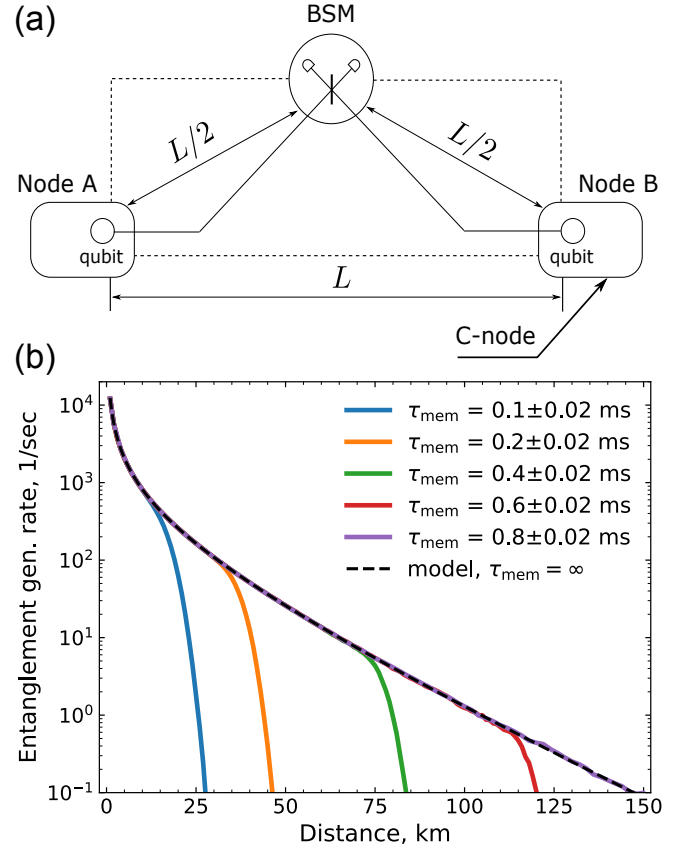


FIG. 1. (a) Schematics of an elementary quantum link implementing Barrett-Kok protocol for entanglement generation. Solid lines correspond to optical fiber connection for quantum information channel, and dashed lines designate connection for classical information. (b) Simulated entanglement generation rate for different memory lifetimes of the qubits using SeQeNCe. The simulations assume the light velocity in the quantum channel and signal velocity in the classical channel $v = 2 \times 10^5$ km/s, photon attenuation rate in quantum channels $\alpha = 0.2$ dB/km, memories efficiency $\mathcal{E}_m = 90\%$ and detectors efficiency $\mathcal{E}_d = 80\%$. The solid line shows the results from the analytical model given by Eq. (4).

stages. At time $t = 0$ one of the nodes that acts as the control node (C-node) sends a message to another node with a timestamp on when they should start the Barrett-Kok protocol. At timestamp $t = L/v$, where v is the photon velocity in optical fiber, the protocol start time is received. Once the message is received, immediately (assuming no delay), the nodes excite their qubits so that the qubit would then be entangled with the photon in the optical cavity it resides in; Photon emission from the cavity happens with the probability \mathcal{E}_m , which is called memory efficiency. At timestamp $t = 2.5L/v$ the leaked photons should reach the BSM station, where the measurement takes place. For simplicity, we assume that the signal speed in the classical channel is v , the same as in the quantum channel, and the lengths of the corresponding quantum and classical optical channels are the same. Thus, the result of measurements in BSM

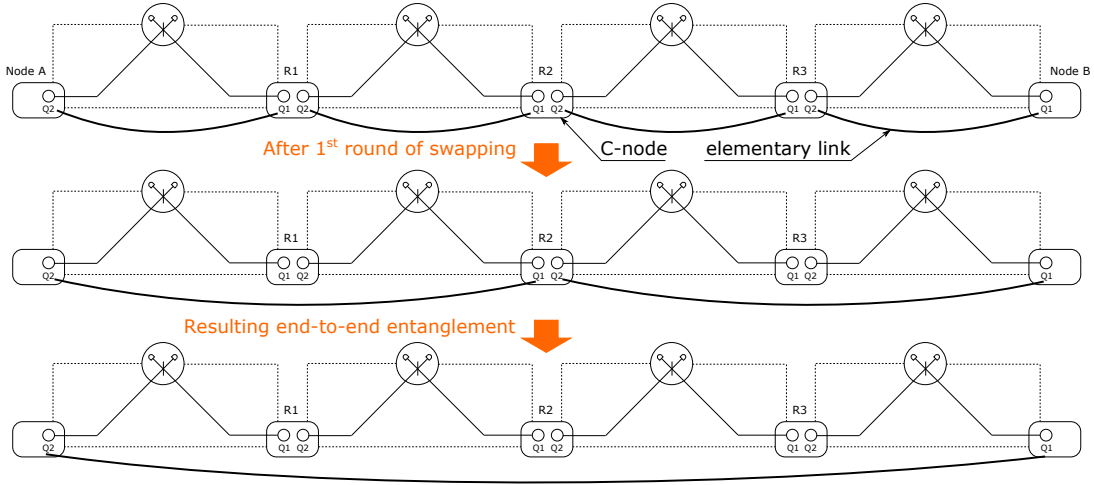


FIG. 2. Schematics of end-nodes connected via three quantum repeaters ($r = 3$) and entanglement swapping iterations resulting in the final entanglement between the end-nodes.

is received at timestamp $t = 3L/v$. Additionally, BSM measurements in the Barrett-Kok protocol are done two times successively, and once results of the second round of measurements are obtained, both nodes know the final result of the entanglement generation attempt at timestamp $t = 4L/v$. If the entanglement is successfully generated, both nodes immediately use it according to their program (e.g., for quantum teleportation or simultaneous measurement in different bases as it requires in the BB84 protocol [51], then we increase the counter of generated entanglements. We assume that at timestamp $t = 4L/v$ the described steps are repeated from the beginning. After escaping their cavities, photons can be lost in fiber due to the attenuation, which we model by the decay probability $e^{-\gamma L/2}$, $\gamma = \alpha/10 \cdot \log 10$, where α is the attenuation constant (given in dB per length) and $L/2$ is the fiber length, as shown in Fig. 1a. The BSM station contains two single-photon detectors, each detecting a photon with probability \mathcal{E}_d that is called detector efficiency. If both photons are detected, only two out of four Bell-states can be measured by this scheme. Ideally, the success rate for the Barrett-Kok protocol for entanglement swapping with BSM is $\mathcal{E}_b = 50\%$ [49]. Including the losses and finite efficiencies of the qubit and the BSM, the total success probability that after the measurement, the qubits of the communicating nodes will be entangled (and BSM detects this) is:

$$P_1(L) = \mathcal{E}_b \mathcal{E}_m^2 \mathcal{E}_d^2 e^{-\gamma L}. \quad (1)$$

Neglecting delays in measurements and formation of the classical messages, it takes $4L/v$ time for one attempt to generate entanglement. The success probability for a single attempt is given by Eq. (1), and success probability for k attempts is given by:

$$P_k = (1 - P_1)^{k-1} P_1. \quad (2)$$

The average number of attempts till success and its stan-

dard deviation is given by:

$$\bar{k} = \frac{1}{P_1}, \quad \sqrt{\delta k^2} = \sqrt{\frac{1}{P_1^2} - \frac{1}{P_1}}, \quad (3)$$

where \bar{f}_k means averaging the function f_k over the probability distribution given by Eq. (2). Practically, $P_1 \ll 1$, so that $\sqrt{\delta k^2} \approx 1/P_1$.

Knowing the time spent on a single attempt $4L/v$ and an average number of attempts till successful entanglement generation, one can calculate how much time on average it takes for one successful entanglement generation. Furthermore, entanglement can exist only for a limited time τ_{mem} , called memory lifetime. If the entanglement degrades too much before the photon reaches BSM, it would be impossible to establish a quantum link between the two nodes. In SeQUeNCe, τ_{mem} is a fixed parameter counting lifetime of an entanglement since its inception when a qubit had successfully entangled with the photon. Once two photons with different scheduled expiration timestamps t_1 and t_2 are successfully measured by BSM, the lifetime for the generated entanglement between the two qubits is equal to $\min\{t_1, t_2\}$. Defining the entanglement generation rate \mathcal{R} as reversed average time spent on the generation of entanglement, one can write the following:

$$\mathcal{R}_0 = \begin{cases} \frac{v}{4L} \mathcal{E}_b \mathcal{E}_m^2 \mathcal{E}_d^2 e^{-\gamma L}, & L < 2v\tau_{\text{mem}}, \\ 0, & L \geq 2v\tau_{\text{mem}}. \end{cases} \quad (4)$$

We assume that the repetition rate for the quantum state preparation is higher than v/L . The former would determine the entanglement generation rate in the $L \rightarrow 0$ limit.

III. END-TO-END QUANTUM CONNECTION IN A NETWORK

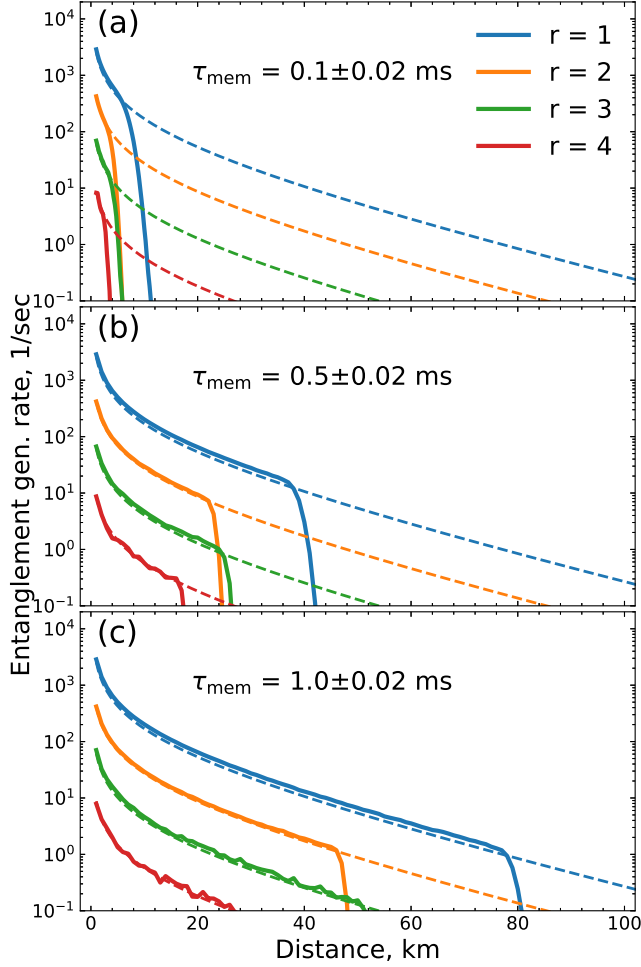


FIG. 3. (solid lines): Simulated with SeQUeNCe entanglement generation rate versus distance between end-nodes for a different number of repeaters and memory lifetimes. Each dashed line is calculated using the analytical model given by Eq. (5) and (6) for the same parameters (but τ_{mem} which in the models is taken as ∞) as solid dependence of the same color. The repeaters are working in synchronous mode (see the text). Entanglement swapping probability is taken as $\mathcal{E}_s = 50\%$. The parameters of quantum memories, BSM, and optical channels are the same as in Fig. 1b: $\mathcal{E}_m = 90\%$, $\mathcal{E}_d = 80\%$, $\alpha = 0.2$ dB/km and $v = 2 \times 10^5$ km/s.

Once an elementary quantum link between the nodes having a direct physical connection is established, it is possible to join elementary links in a longer end-to-end quantum link using the entanglement swapping protocol (see Fig. 2) [52]. If one needs to establish the end-to-end connection between some pairs of distant nodes, then some algorithms would choose the optimal path from one end-node to another via intermediate nodes, which are considered quantum routers. Once the path is deter-

mined, the problem of establishing the end-to-end connection is reduced to establishing connections between the nodes in a chain of successive nodes (or quantum routers). Quantum routers give us dual benefits. The first one allows us to achieve connectivity by a much smaller number of physical communication links between the nodes than $N(N-1)/2$, where the N is the number of nodes in the network. The second one is the overcoming (in some cases) exponential factor in Eq. (4). In the case of a network, L in Eq. (4) is the communication path length between the end nodes. To recover the entanglement/fidelity losses, we divide the distance between the end nodes A and B into several segments by setting up a number r of intermediate nodes (or quantum repeaters), as shown in Fig. 2) for the case of $r = 3$. For simplicity, we consider only a chain-like topology of the networks with equal distances between the adjacent nodes and generation end-to-end quantum connectivity between the end nodes.

Suppose all the links between adjacent qubits in Fig. 2 are established. The next step is to perform entanglement swapping [52] within each of the repeater nodes simultaneously, which would allow qubits in the end nodes to become entangled if all the swappings are successful. The time duration for this process is spent on two kinds of procedures. The first one, for the nodes in the middle to acknowledge to the side nodes containing entangled qubits about the result of the swapping. The second procedure, for all the nodes involved in the swapping to acknowledge the C-node about the operation results. The total time spent on the entanglement swapping can be approximately expressed as $\tilde{n}L/2v$, where $\tilde{n} = \log_2(r+1)$ is the number of stages at which the total entanglement swapping procedure is done. That derivation assumes that the number of repeaters equals to $r = 2^{\tilde{n}} - 1$. In Fig. 4 we demonstrate a case of $r = 3$, which would require $\tilde{n} = 2$ stages to establish entanglement between the end nodes. However, we find little deviations between the analytical expression and the numerical simulations even for the cases when \tilde{n} is not an integer.

The probability of success of swapping operation is \mathcal{E}_s . If swapping fails at any of the elementary links, the whole process fails, and all the links between the adjacent nodes must be discarded and re-generated. This is because when a particular swapping fails, the rest of the links are not as *fresh* as newly generated anymore. If the established links had to wait for the regeneration of the broken links, they would have degraded further and become less reliable. Thus, everything has to be done from scratch in this approach if one link is not established successfully. The whole process is repeated until entanglement between the end-nodes is established.

1. Synchronous generation of entanglements between adjacent nodes

Now let us consider the case of entanglement generation with r repeaters and $r+1$ elementary links, where we try to generate entanglement between adjacent repeater nodes simultaneously and discard everything if one link generation fails. In such a scheme, we obtain the *freshest* entanglement because the entanglement between adjacent nodes is established at the same time. There is no need for any waiting. Due to the shorter lengths between neighboring repeater nodes, their presence decreases the total time needed for one generation try, which is now to $3L/(v(r+1)) + L/v$. Here we neglect the time needed for entanglement swapping but take into account the time needed for the C-node (in the middle of the repeaters chain) to inform all the nodes about the start time of synchronous entanglement generation and the time needed for the nodes to return their elementary link generation status to the C-node. The probability of successful generation of all the links simultaneously and swapping all of them equals to $\mathcal{E}_s^r [P_1 (L/[r+1])]^{r+1}$, which gives the following generation rate for the entanglement:

$$\mathcal{R}_{\text{syn}} = \frac{v}{L} \left[\frac{3}{r+1} + 1 \right]^{-1} \mathcal{E}_b^{r+1} \mathcal{E}_s^r (\mathcal{E}_m \mathcal{E}_d)^{2(r+1)} e^{-\gamma L}. \quad (5)$$

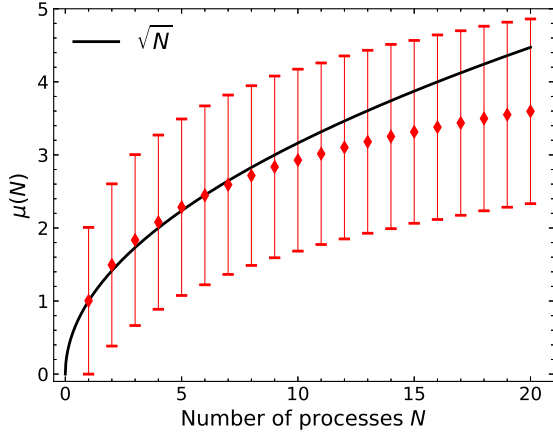


FIG. 4. Averaged over 10^6 repetitions $\max k_i, i = 1 \dots N$ versus the size of query N , where k_i are N random values generated by the distribution given in Eq. (2). Parameter of the distribution $P_1 = 10^{-3}$. The result is normalized to $\bar{k} = 1/P_1$. Error bars show a standard deviation of $\max k_i$.

For simplicity, when analyzing the cases with an arbitrary number of repeaters, we do not bring the memory coherence time into an analytical expression Eq. (5). However, we should keep in mind that the described scheme, despite its efficiency in saving *freshness* of the generated entanglements, cannot overcome the limit imposed by the distance between the end nodes of $\lesssim 0.5v\tau_{\text{mem}}$. Otherwise, the entangled memories would degrade during a photon travel time of about $2L/v/(r+1) +$

$\tilde{n}L/v$ ($2L/v/(r+1)$) as in the no-repeater case. There is also the time of about $\tilde{n}L/v$ while the C-nodes wait for the confirmation that the end nodes are ready for entanglement swapping and while the entanglement swapping proceeds.

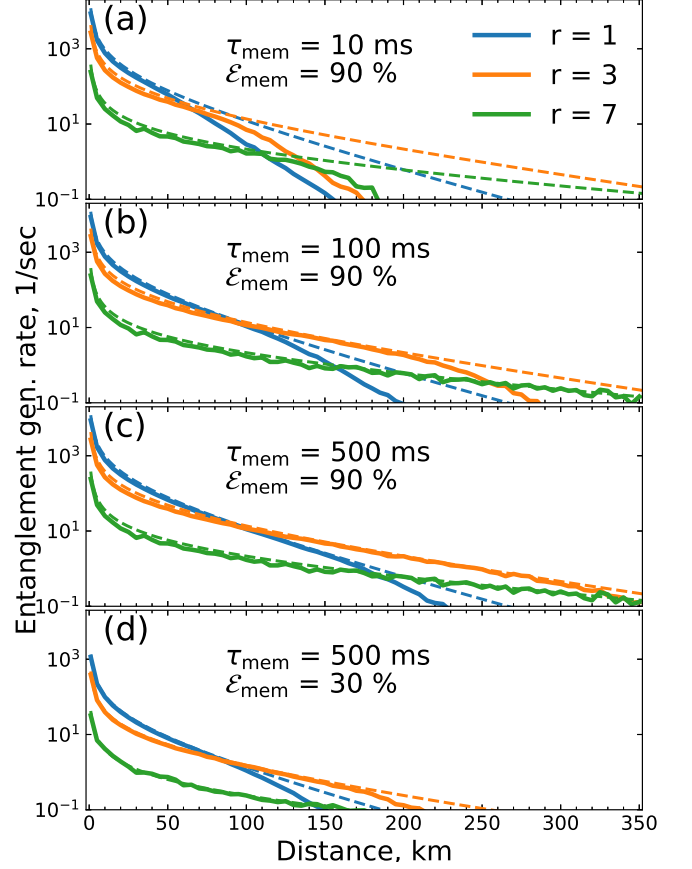


FIG. 5. The same dependencies as in Fig. 3 but simulated with SeQUeNCe (solid lines) and calculated analytically with Eq. (6) for different memories lifetime and in independent (see the text) mode of elementary links generation. Each dashed line is calculated using the analytical model for the same parameters (but τ_{mem} which in the models is taken as ∞) as solid dependence of the same color. All but memories lifetime parameters (\mathcal{E}_s , \mathcal{E}_m , \mathcal{E}_d , α and v) are the same as in the case of Fig. 3 except for panel (d), where we used a smaller memory efficiency $\mathcal{E}_m = 30\%$.

Equation (5) was derived in the limit when the probability of photon loss in a quantum channel is very low. In this case, the most probable outcome of generation attempt is a failure and the outcomes whose duration is longer than $3L/(v(r+1)) + L/v$ are negligible. However, plots in Fig. 3 show that this assumption is also applicable in the cases of relatively short distances between the end-nodes, of about $\gtrsim 1$ km. The minor discrepancies between Eq. (5) and the numerical simulations are caused by the lack of path optimization notifying signal sent to the C-node from the nodes generating elementary links. In other words, we assume that the notification is

sent only by the node that is closer to the C-node. Thus, the time delay between the Barrett-Kok protocol operation while generating the elementary links instead of L/v should be less at least by about $L/v/(r+1)$. Taking into account that we also simulate cases when $r+1 \neq 2^l$, $l \in \mathcal{N}$, consequently, C-node is not exactly in the middle of the chain. A more precise version of Eq. (5) is significantly more complicated. Thus we keep the current form not to burden the readers with technical details.

As shown in Eq. (5), one feature of synchronous entanglement generation is that it gives an even lower entanglement generation rate than in the no-repeater case. However, such a scheme allows to utilize the intermediate nodes as routers and organize multiple nodes into a quantum network without the need to lay communication fiber between each pair of the network nodes.

2. Independent generation of entanglements between adjacent nodes

Another way to generate an entanglement link between end nodes allows all the adjacent repeater nodes to generate their links independently until success, without discarding already established ones. In this scheme, a complete link between end nodes can be generated much faster than the synchronous protocol, though each repeater link has its own time of creation. Consequently, some of the links that are established early on would have to wait for a long time, making decoherence a much more significant issue than in the synchronous protocol. This is evident in our numerical simulation: the longer the time difference between the links completed first and the last, the more probabilistic events are tested, the wider histogram is obtained.

We simulate a set of N processes determined by the distribution given in Eq. (2) using pseudo-random number generation. Each of the processes gives its own number of stages k_i till completion in accordance to Eq. (2), then the resulting value $\mu(N)$ is obtained as $\max k_i$ (see Eq. (3)) is averaged over about 10^6 repetitions and normalized to \bar{k} . Figure 4 shows the result for the distribution parameter $P_1 \lesssim 0.001$, but for so small P_1 the plot doesn't depend on P_1 .

For $N \leq 8$, the obtained dependence can be approximated well as $\mu(N) \approx \sqrt{N}$. Therefore, in the case when $r+1$ entanglements are generated by the pairs of nodes independently, the average number of tries till the last link is generated is $\mu(r+1)/P_1$. Analogously to Eqs. (4) and (5), one can obtain an entanglement generation rate proportional to $P_1(L/[r+1])$ in this scheme:

$$\mathcal{R}_{\text{ind}} = \left[\frac{3\mu(r+1)}{r+1} \right]^{-1} \frac{v}{L} \mathcal{E}_b \mathcal{E}_s^r \mathcal{E}_m^2 \mathcal{E}_d^2 e^{-\gamma L/(r+1)}. \quad (6)$$

The average "age" of the oldest entangled memory by the time when the end-to-end entanglement is established is:

$$\Delta t = \mathcal{R}_{\text{ind}}^{-1} + \frac{L}{v} \log_2(r+1). \quad (7)$$

From the previous two equations, $\Delta t \gg L/v$ since the contribution from the entanglement generation rate \mathcal{R}_{ind} should dominate in Δt . Consequently, quantum memory lifetime should be at least $\tau_{\text{mem}} \gtrsim \Delta t$. However, the simulations in Fig. 5 show that after $\mathcal{R}_{\text{ind}}^{-1}$ reaches approximately τ_{mem}^{-1} , the entanglement generation rate starts to degrade faster, though not as rapidly as in the synchronous scheme considered in the previous section.

Fig. 5 demonstrates that in the limit of long memory lifetime, Eq. (6) works very well for predicting entanglement generation rate as a function of distance, a number of repeaters, and parameters defining hardware performance. Therefore, a reverse problem of finding the required parameters of the QLAN hardware components for a given distance and entanglement generation rate can be solved.

IV. CONCLUSIONS

We have simulated two types of protocols of elementary quantum links in a chain-like network supporting quantum entanglement between the end-nodes. The hardware components and basic protocols for entanglement generation and swapping are adopted from the SeQUeNCe package. We have explored the effects of finite memory lifetime on entanglement generation in a quantum network and considered two entanglement swapping protocols. For the synchronous generation of entanglement between adjacent nodes, the advantages of a quantum repeater are limited. On the other hand, for the independent generation of entanglement between adjacent nodes, additional repeaters enable communication at longer distances between the end nodes. We present analytical solutions for the entanglement generation rate for both scenarios applicable for infinitely long quantum memory lifetimes. In both cases, our numerical simulations demonstrate that entanglement generation degrades due to a finite quantum memory lifetime, whereas this degradation is less severe in the independent generation of entanglements scenario. Our results demonstrate the ultimate performance of a quantum network as a function of the performance of the network's hardware components, the number of repeaters, the distance between the end nodes, and the lifetime of the quantum memories.

ACKNOWLEDGMENTS

We gratefully acknowledge Kathy-Anne Soderberg and David Hucul from AFRL lab in Rome, NY, for insightful discussions and funding from the Vice President for Research and Economic Development (VPRED) and SUNY Research Seed Grant Program, and computational facilities at the Center for Computational Research at the University at Buffalo (<http://hdl.handle.net/10477/79221>).

-
- [1] Sangouard, N.; Simon, C.; de Riedmatten, H.; Gisin, N. Quantum repeaters based on atomic ensembles and linear optics. *Rev. Mod. Phys.* **2011**, *83*, 33–80.
- [2] Bao, X.-H.; Reingruber, A.; Dietrich, P.; Rui, J.; Dück, A.; Strassel, T.; Li, L.; Liu, N.-L.; Zhao, B.; Pan, J.-W. Efficient and long-lived quantum memory with cold atoms inside a ring cavity. *Nature Phys.* **2012**, *8*, 517–521.
- [3] Chen, Z.-B.; Zhao, B.; Chen, Y.-A.; Schmiedmayer, J.; Pan, J.-W. Fault-tolerant quantum repeater with atomic ensembles and linear optics. *Phys. Rev. A* **2007**, *76*, 022329.
- [4] Jin, R.-B.; Takeoka, M.; Takagi, U.; Shimizu, R.; Sasaki, M. Highly efficient entanglement swapping and teleportation at telecom wavelength. *Phys. Rev. Lett.* **2015**, *5*, 9333.
- [5] Sun, Q.-C.; Jiang, Y.-F.; Mao, Y.-L.; You, L.-X.; Zhang, W.; Zhang, W.-J.; Jiang, X.; Chen, T.-Y.; Li, H.; Huang, Y.-D.; Chen, X.-F.; Wang, Z.; Fan, J.; Zhang, Q.; Pan, J.-W. Entanglement swapping over 100 km optical fiber with independent entangled photon-pair sources. *Optica* **2017**, *4*, 1214.
- [6] van Leent, T.; Bock, M.; Garthoff, R.; Redeker, K.; Zhang, W.; Bauer, T.; Rosenfeld, W.; Becher, C.; Weinfurter, H. Long-Distance Distribution of Atom-Photon Entanglement at Telecom Wavelength. *Phys. Rev. Lett.* **2020**, *124*, 010510.
- [7] Dideriksen, K. B.; Schmieg, R.; Zugenmaier, M.; Polzik, E. S. Room-temperature single-photon source with near-millisecond built-in memory. *Nature Commun.* **2021**, *12*, 3699.
- [8] Pompili, M.; Hermans, S. L. N.; Baier, S.; Beukers, H. K. C.; Humphreys, P. C.; Schouten, R. N.; Vermeulen, R. F. L.; Tiggelman, M. J.; Dos Santos Martins, L.; Dirkse, W. S., B.; Hanson, R. Highly efficient entanglement swapping and teleportation at telecom wavelength. *Science* **2021**, *372*, 259–264.
- [9] Duan, L.-M.; Lukin, M. D.; Cirac, J. I.; Zoller, P. Long-distance quantum communication with atomic ensembles and linear optics. *Nature* **2001**, *414*, 413–418.
- [10] Wang, X.-J.; Yang, S.-J.; Sun, P.-F.; Jing, B.; Li, J.; Zhou, M.-T.; Bao, X.-H.; Pan, J.-W. Cavity-Enhanced Atom-Photon Entanglement with Subsecond Lifetime. *Phys. Rev. Lett.* **2021**, *126*, 090501.
- [11] Du, D.; Stankus, P.; Saira, O.-P.; Flament, M.; Sagona-Stophel, S.; Namazi, M.; Katramatos, D.; Figueroa, E. An elementary 158 km long quantum network connecting room temperature quantum memories. 2021.
- [12] Muralidharan, S.; Li, L.; Kim, J.; Lütkenhaus, N.; Lukin, M. D.; Jiang, L. Optimal architectures for long distance quantum communication. *Scientific Reports* **2016**, *6*, 20463.
- [13] Flamini, F.; Spagnolo, N.; Sciarrino, F. **2018**, *82*, 016001.
- [14] Muralidharan, S.; Li, L.; Kim, J.; Lütkenhaus, N.; Lukin, M. D.; Jiang, L. Optimal architectures for long distance quantum communication. *Scientific Reports* **2016**, *6*, 20463.
- [15] Wehner, S.; Elkouss, D.; Hanson, R. Quantum internet: A vision for the road ahead. *Science* **2018**, *362*, eaam9288.
- [16] Simon, C.; de Riedmatten, H.; Afzelius, M.; Sangouard, N.; Zbinden, H.; Gisin, N. Quantum Repeaters with Photon Pair Sources and Multimode Memories. *Phys. Rev. Lett.* **2007**, *98*, 190503.
- [17] Sinclair, N.; Saglamyurek, E.; Mallahzadeh, H.; Slater, J. A.; George, M.; Ricken, R.; Hedges, M. P.; Oblak, D.; Simon, C.; Sohler, W.; Tittel, W. Spectral Multiplexing for Scalable Quantum Photonics using an Atomic Frequency Comb Quantum Memory and Feed-Forward Control. *Phys. Rev. Lett.* **2014**, *113*, 053603.
- [18] Guha, S.; Krovi, H.; Fuchs, C. A.; Dutton, Z.; Slater, J. A.; Simon, C.; Tittel, W. Rate-loss analysis of an efficient quantum repeater architecture. *Phys. Rev. A* **2015**, *92*, 022357.
- [19] Wu, Y.; Liu, J.; Simon, C. Near-term performance of quantum repeaters with imperfect ensemble-based quantum memories. *Phys. Rev. A* **2020**, *101*, 042301.
- [20] Vardoyan, G.; Guha, S.; Nain, P.; Towsley, D. On the Stochastic Analysis of a Quantum Entanglement Distribution Switch. *IEEE Transactions on Quantum Engineering* **2021**, *2*, 1–16.
- [21] Jing, B.; Wang, X.-J.; Yu, Y.; Sun, P.-F.; Jiang, Y.; Yang, S.-J.; Jiang, W.-H.; Luo, X.-Y.; Zhang, J.; Jiang, X.; Bao, X.-H.; Pan, J.-W. Entanglement of three quantum memories via interference of three single photons. *Nature Photon.* **2019**, *13*, 210–213.
- [22] Bock, M.; Eich, P.; Kucera, S.; Kreis, M.; Lenhard, A.; Becher, C.; Eschner, J. High-fidelity entanglement between a trapped ion and a telecom photon via quantum frequency conversion. *Nature Commun.* **2018**, *9*, 1998.
- [23] Yu, Y. et al. Entanglement of two quantum memories via fibres over dozens of kilometres. *Nature* **2020**, *578*, 240–245.
- [24] Yang, S.-J.; Wang, X.-J.; Bao, X.-H.; Pan, J.-W. . An efficient quantum light–matter interface with sub-second lifetime. *Nature Photon.* **2016**, *10*, 381–384.
- [25] Bhaskar, M. K.; Riedinger, R.; Machielse, B.; Levonian, D. S.; Nguyen, C. T.; Knall, E. N.; Park, H.; Englund, D.; Lončar, M.; Sukachev, D. D.; Lukin, M. D. Experimental demonstration of memory-enhanced quantum communication. *Nature* **2020**, *580*, 60–64.
- [26] Hanson, R.; Kouwenhoven, L. P.; Petta, J. R.; Tarucha, S.; Vandersypen, L. M. K. Spins in few-electron quantum dots. *Rev. Mod. Phys.* **2007**, *79*, 1217–1265.
- [27] Pla, J. J.; Tan, K. Y.; Dehollain, J. P.; Lim, W. H.; Morton, J. J. L.; Zwanenburg, F. A.; Jamieson, D. N.; Dzurak, A. S.; Morello, A. High-fidelity readout and control of a nuclear spin qubit in silicon. *Nature* **2013**, *496*, 334–338.
- [28] Balasubramanian, G.; Neumann, P.; Twitchen, D.; Markham, M.; Kolesov, R.; Mizuochi, N.; Isoya, J.; Achard, J.; Beck, J.; Tissler, J.; Jacques, V.; Hemmer, P. R.; Jelezko, F.; Wrachtrup, J. Ultralong spin coherence time in isotopically engineered diamond. *Nature* **2009**, *457*, 868–871.
- [29] Awschalom, D. D.; Hanson, R.; Wrachtrup, J.; Zhou, B. B. Quantum technologies with optically interfaced solid-state spins. *Nature Nanotechnol.* **2014**, *9*, 793–801.
- [30] Abobeih, M. H.; Cramer, J.; Bakker, M. A.; Kalb, N.; Markham, M.; Twitchen, D. J.; Taminiau, T. H. One-second coherence for a single electron spin coupled to a multi-qubit nuclear-spin environment. *Nat. Commun.* **2019**, *10*, 1111.

- 2018**, *9*, 2552.
- [31] Langer, C. et al. Long-Lived Qubit Memory Using Atomic Ions. *Phys. Rev. Lett.* **2005**, *95*, 060502.
 - [32] Kotler, S.; Akerman, N.; Navon, N.; Glickman, Y.; Ozeri, R. Measurement of the magnetic interaction between two bound electrons of two separate ions. *Nature* **2014**, *510*, 376–380.
 - [33] Wang, P.; Luan, C.-Y.; Qiao, M.; Um, M.; Zhang, J.; Wang, Y.; Yuan, X.; Gu, M.; Zhang, J.; Kim, K. Single ion qubit with estimated coherence time exceeding one hour. *Nature Commun.* **2021**, *12*, 233.
 - [34] Kwiat, P. G.; Mattle, K.; Weinfurter, H.; Zeilinger, A.; Sergienko, A. V.; Shih, Y. New High-Intensity Source of Polarization-Entangled Photon Pairs. *Phys. Rev. Lett.* **1995**, *75*, 4337–4341.
 - [35] Boyd, R. W. *Nonlinear Optics, Third Edition*, 3rd ed.; Academic Press, Inc.: USA, 2008.
 - [36] Schneeloch, J.; Knarr, S. H.; Bogorin, D. F.; Levangie, M. L.; Tison, C. C.; Frank, R.; Howland, G. A.; Fanto, M. L.; Alsing, P. M. Introduction to the absolute brightness and number statistics in spontaneous parametric down-conversion. *Journal of Optics* **2019**, *21*, 043501.
 - [37] Zhao, H.; Pettes, M. T.; Yu Zheng, H. H. Site-Controlled Telecom Single-Photon Emitters in Atomically-thin MoTe₂. *arXiv:2105.00576* **2021**,
 - [38] Saglamyurek, E.; Jin, J.; Verma, V. B.; Shaw, M. D.; Marsili, F.; Nam, S. W.; Oblak, D.; Tittel, W. Quantum storage of entangled telecom-wavelength photons in an erbium-doped optical fibre. *Nature Photon.* **2015**, 83–87.
 - [39] Lago-Rivera, D.; Grandi, S.; Rakonjac, J. V.; Seri, A.; de Riedmatten, H. Telecom-heralded entanglement between multimode solid-state quantum memories. *Nature* **2021**, *594*, 37–40.
 - [40] Kim, J.-H.; Aghaieimebodi, S.; Richardson, C. J. K.; Leavitt, R. P.; Englund, D.; Waks, E. Hybrid Integration of Solid-State Quantum Emitters on a Silicon Photonic Chip. *Nano Lett.* **2017**,
 - [41] Singh, M. K.; Jiang, L.; Awschalom, D. D.; Guha, S. Key Device and Materials Specifications for a Repeater Enabled Quantum Internet. *IEEE Transactions on Quantum Engineering* **2021**, *2*, 1–9.
 - [42] Dahlberg, A.; Wehner, S. SimulaQron—a simulator for developing quantum internet software. *Quantum Science and Technology* **2018**, *4*, 015001.
 - [43] Wu, X.; Chung, J.; Kolar, A.; Wang, E.; Zhong, T.; Kettimuthu, R.; Suchara, M. Simulations of Photonic Quantum Networks for Performance Analysis and Experiment Design. 2019 IEEE/ACM Workshop on Photonics-Optics Technology Oriented Networking, Information and Computing Systems (PHOTONICS). 2019; pp 28–35.
 - [44] Matsuo, T. Simulation of a Dynamic, RuleSet-based Quantum Network. 2019.
 - [45] Wu, X.; Kolar, A.; Chung, J.; Jin, D.; Zhong, T.; Kettimuthu, R.; Suchara, M. SeQUeNCe: A Customizable Discrete-Event Simulator of Quantum Networks. *arXiv:2009.12000* **2020**,
 - [46] Coopmans, T. et al. NetSquid, a NETwork Simulator for QUantum Information using Discrete events. *Communications Physics* **2021**, *4*, 164.
 - [47] Diadamo, S.; Nötzel, J.; Zanger, B.; Beşe, M. M. QuNet-Sim: A Software Framework for Quantum Networks. *IEEE Transactions on Quantum Engineering* **2021**, *2*, 1–12.
 - [48] Harty, T. P.; Allcock, D. T. C.; Ballance, C. J.; Guidoni, L.; Janacek, H. A.; Linke, N. M.; Stacey, D. N.; Lucas, D. M. High-Fidelity Preparation, Gates, Memory, and Readout of a Trapped-Ion Quantum Bit. *Phys. Rev. Lett.* **2014**, *113*, 220501.
 - [49] Barrett, S. D.; Kok, P. Efficient high-fidelity quantum computation using matter qubits and linear optics. *Phys. Rev. A* **2005**, *71*, 060310.
 - [50] Vu, Q. H.; Lupu, M.; Ooi, B. C. *Peer-to-Peer Computing: Principles and Applications*; Springer-Verlag Berlin Heidelberg, 2010.
 - [51] Bennett, C. H.; Brassard, G. Quantum cryptography: Public key distribution and coin tossing. *Theoretical Computer Science* **2014**, *560*, 7–11, Theoretical Aspects of Quantum Cryptography – celebrating 30 years of BB84.
 - [52] Asadi, F. K.; Wein, S. C.; Simon, C. Protocols for long-distance quantum communication with single ¹⁶⁷Er ions. *Quantum Science and Technology* **2020**, *5*, 045015.